RESEARCH ARTICLE



WILEY

The role of indium composition in In_xGa_{1-x}N prestrained layer towards optical characteristics of EBL free GaN/InGaN nanowire LEDs for enhanced luminescence

Samadrita Das¹ | Trupti Ranjan Lenka¹ | Fazal Ahmed Talukdar¹ Hieu Pham Trung Nguyen² | Giovanni Crupi³

Correspondence

Trupti Ranjan Lenka, Department of Electronics and Communication Engineering, National Institute of Technology Silchar, Silchar, Assam 788010. India.

Email: trlenka@ieee.org

Funding information

Science and Engineering Research Board, Grant/Award Number: MTR/2021/000370

Abstract

In this work, an electron blocking layer (EBL) free light emitting diode (LED) nanowire is proposed with alternate prestrained layers of In_xGa_{1-x}N/GaN, which are inserted between the GaN/InGaN multi-quantum wells (MQWs) and n-GaN layer. This study signifies the role of prestrained layers on the piezoelectric polarization of LED nanowires, for enhanced luminescence. When compared with the conventional one, the EBL free LED nanowire with prestrained layer shows an enhancement of ~2.897% efficiency, which occurs due to the reduction of polarization field in the active region. The LED with 15% indium in the prestrained layer obtains a maximum efficiency of 85.21% along with a minimum efficiency droop of 3.848% at 40 mA injected current. The proposed III-nitride LED nanostructure allows for achieving superior optical power across the output spectral range.

KEYWORDS

electron blocking layer (EBL), GaN, LED, multi-quantum well (MQW), quantum-confined Stark effect (QCSE)

1 INTRODUCTION

Group III-nitride ultraviolet (UV) light emitting diodes (LEDs) have attained remarkable attention as a suitable and eco-friendly light source for various applications, such as pharmaceutical applications, water and air purification, surface disinfection, displays, and so forth. In the UV wavelength range, LEDs are used in a broad range of applications, such as water purification, sterilization, chemical and bio-chemical sensing, smart sensor networks, advanced manufacturing, and many more. 1,2 Various works on LEDs have been reported, such as InGaN LEDs used in an optical link,³ parallel flip-chip AlGaN LED whose electrical and optical characteristics display strong size dependence for communication in the UV range,⁴ and introduction of light-emitting commutating diodes (LECDs).⁵ III-nitride materials are capable of manufacturing lasers and LEDs, 6,7 but it is still difficult to get high efficiency GaN/InGaN LED. The strong piezoelectric polarization (PZ), along the c-plane direction, induced by high lattice mismatch within GaN and InGaN layers causes the quantum-confined Stark effect (QCSE)8 which eventually causes reduction of device's efficiency (EQE).^{9,10} However the Stark effect is not preferable as it causes notable spatial separation of the carrier wave functions. 11-13

From the past research, prestrained growth method plays a crucial role for improving the efficiency of GaN/InGaN multi-quantum wells (MQWs).¹⁴ While depositing of the prestrain layers before the MQW, a tensile strain is created in

¹Department of Electronics and Communication Engineering, National Institute of Technology Silchar, Silchar, Assam, India

²Department of Electrical and Computer Engineering, Texas Tech University, Lubbock, Texas, USA

³BIOMORF Department, University of Messina, Messina, Italy

DAS ET AL.

.0991.204, 2024, 2, Downloaded from https://onlinelibrary.wiley.com/doi/10.1002/jnm.3169 by National Yang Ming Chiao Tung University, Wiley Online Library on [30.06/2024]. See the Terms and Conditions (https://online.library.online).

the quantum barrier, 15 thus enhancing the incorporation of large sized indium atoms. Consequently, this leads to the reduction of OCSE.14

Here, we have studied about strain relaxation in an electron blocking layer (EBL) free MQW LED nanowire when we have examined the role of varying indium composition contained in the prestrained layers. The proposed LED device consists of high indium composition and is based on silicon substrate.

The paper is structured as follows. Section 2 discusses about device structure and simulation methodology. Next, the results are discussed in Section 3. Finally, the conclusions are provided in Section 4.

2 DEVICE PARAMETERS AND NANO STRUCTURE

The computer-aided software Silvaco TCAD is used to study the role of prestrained InGaN interlayer in an EBL free LED nanowire. 16

In this study, three LED nanowires are designed and their performance is scrutinized. The regular nanowire LED (LED₁) comprises of 1-μm undoped GaN buffer layer grown on sapphire substrate, 1.8-μm n-AlGaN (Si doping concentration: $1.5 \times 10^{20} \,\mathrm{cm}^{-3}$), active region with four quantum wells (InGaN: 4nm and 20% indium) and barriers (GaN: 9 nm), EBL of p-AlGaN (20 nm, Mg doping concentration: $2.5 \times 10^{18} \, \mathrm{cm}^{-3}$ and 16% aluminum), 60-nm p-AlGaN cladding layer, and finally 80-nm p-GaN layer. The Shockley-Read-Hall recombination lifetime, radiative, Auger recombination coefficient, light extraction efficiency are taken as $15 \,\mathrm{ns}$, $2.13 \times 10^{-11} \,\mathrm{cm}^3/\mathrm{s}$, $2.88 \times 10^{-30} \,\mathrm{cm}^6/\mathrm{s}$, and 15%, respectively. 17

In order to obtain minimal strain and less PZ effect, we have modified the conventional device LED₁ by inserting 4-pairs of InGaN/GaN prestrain layer with 0.06 indium composition prior to the active region. This modified nanowire LED is denoted as LED₂ in our context. However, to nullify the electron leakage affect, the EBL is now removed from LED₂ and this proposed designed is represented as LED₃ (see Figure 1). LED₃ has a nominal indium composition of 0.15 in the prestrain layer.

From the energy band diagrams in Figure 2, the effective conduction band barrier height (CBBH) and valence band barrier height (VBBH) are observed and numerical study on the three LEDs are performed. The effective CBBH at the corresponding barrier (n) and EBL layer are denoted as $\Phi_{\rm en}$ and $\Phi_{\rm EBL}$, respectively. Similarly, the effective VBBH at the corresponding barrier (n) is represented by $\Phi_{\rm hn}$. Each value from the energy band is listed in Tables 1 and 2. In LED₂ and LED₃, $\Phi_{\rm en}$ is gradually increasing with each barrier and thus prevents the overflow of electrons from jumping

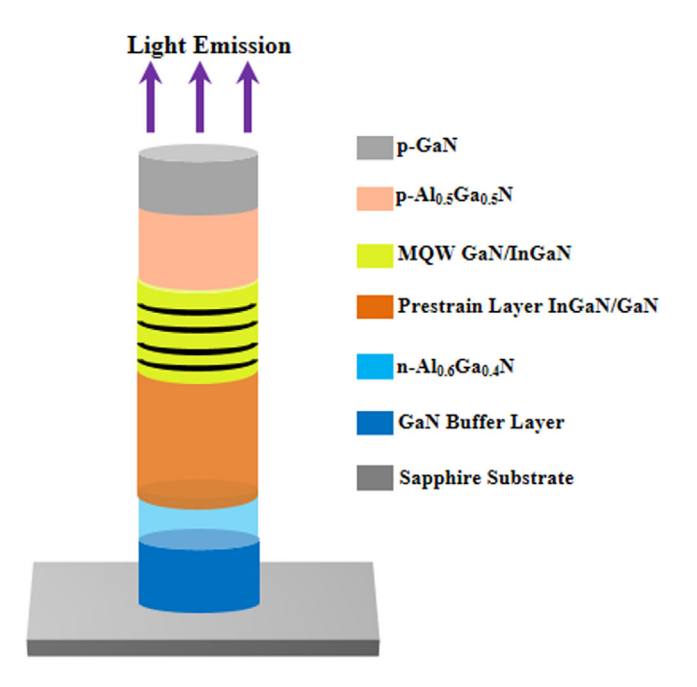


FIGURE 1 Schematic diagrams of the proposed electron blocking layer free GaN/InGaN multi-quantum well (MQW) light emitting diode (LED) (LED3) with InGaN/GaN prestrained layer.

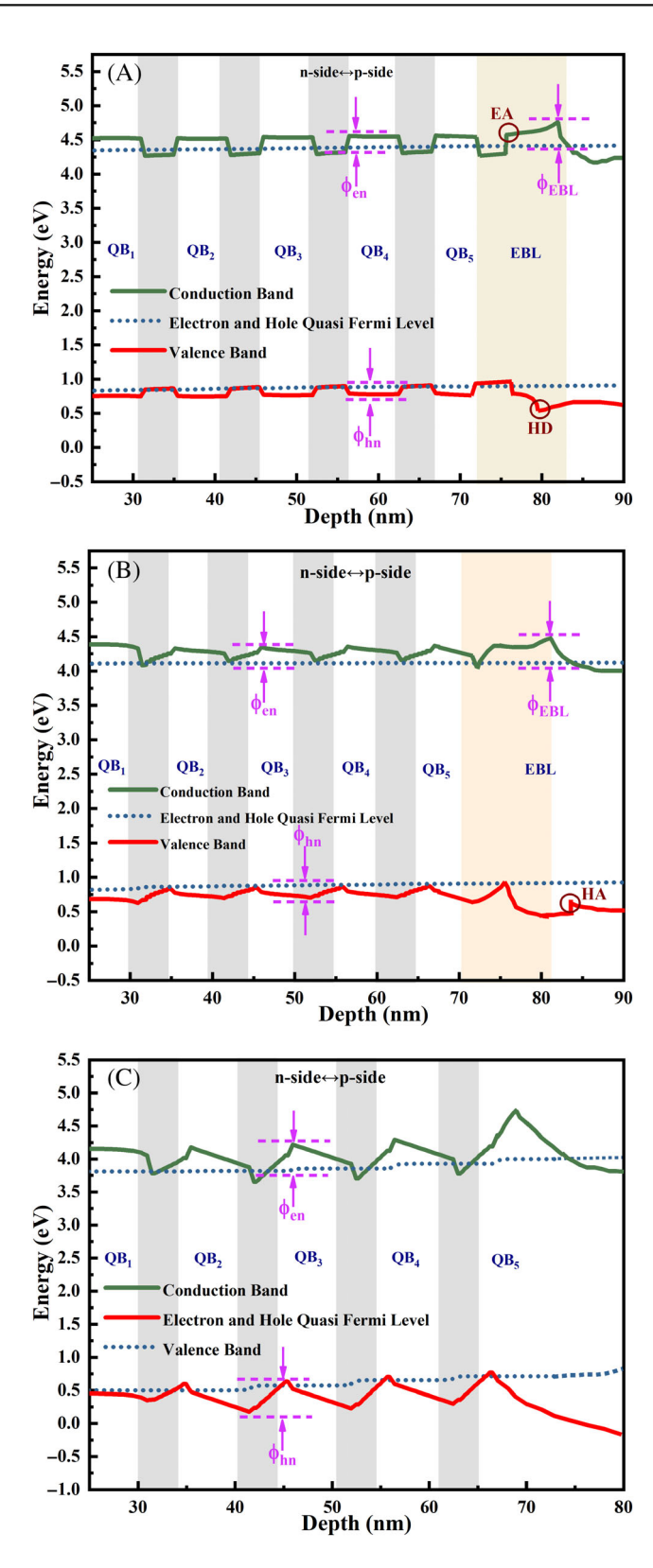


FIGURE 2 Band diagram of (A) conventional LED₁ (B) LED₂, and (C) LED₃. Electron accumulation (EA), hole depletion (HD), and hole accumulation (HA) regions are shown in the figures.

out of the wells. Additionally, Φ_{en} in LED₃ is higher than LED₂ indicating that LED₃ is the suitable choice to trap the electrons in the MQW. The high values of Φ_{hn} in LED₂ and LED₃ indicate the improved hole confinement and increased hole concentration in the active region.

.com/doi/10.1002/jnm.3169 by National Yang Ming Chiao Tung University, Wiley Online Library on [30/06/2024]. See

rules of use; OA articles are governed by the applicable Creative Common:

TABLE 1 Effective conduction band barrier height (CBBH) (in meV) in quantum barriers (Φ_{en}) and electron blocking layer (EBL) (Φ_{EBL}) of LED₁, LED₂, and LED₃.

СВВН	LED_1	LED_2	LED_3
$arPhi_{ m e1}$	174.43	274.67	339.24
$\Phi_{ m e2}$	157.89	217.51	363.19
$oldsymbol{\Phi}_{ ext{e}3}$	162.38	228.23	385.34
$\Phi_{ m e4}$	166.46	238.19	392.93
$arPhi_{ m EBL}$	342.94	524.79	-

Abbreviation: LED, light emitting diode.

TABLE 2 Effective valence band barrier height (VBBH) (in meV) of QBs (Φ_{hn}) for LED₁, LED₂, and LED₃.

VBBH	LED_1	LED_2	LED ₃
$arPhi_{ m h1}$	89.55	145.76	212.05
$arPhi_{ m h2}$	109.94	175.36	336.10
$arPhi_{ m h3}$	110.37	172.99	358.01
$arPhi_{ m h4}$	110.54	186.11	337.69

Abbreviation: LED, light emitting diode.

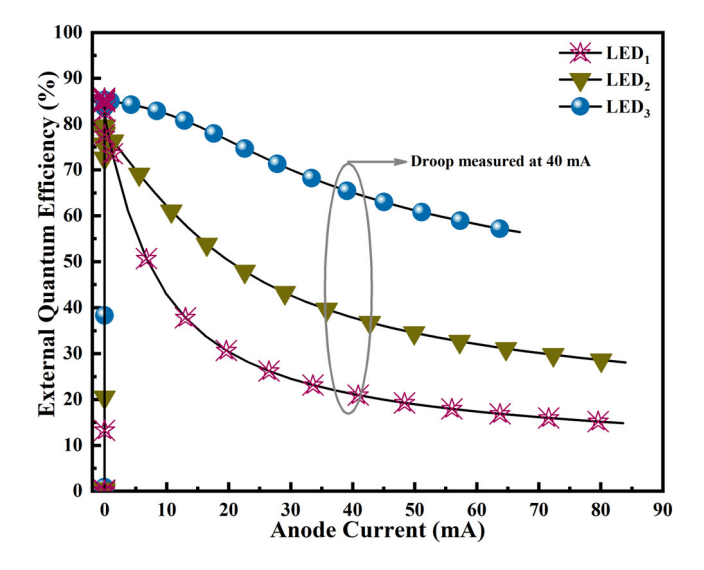


FIGURE 3 External quantum efficiency (EQE) versus anode current for all the three designed light emitting diodes (LEDs).

3 | RESULTS AND DISCUSSION

3.1 | External quantum efficiency

The varying efficiencies for designed samples are shown in Figure 3. EQE can be expressed as shown below which indicates a decrease of efficiency with increase in current¹⁸:

$$IQE = \frac{P/h\nu}{I/e},$$

where P, power; $h\nu$, photon energy emitted; I, injection current; and e, electronic charge. From the graph, LED₃ has the maximum efficiency of 85.22% and a high efficiency of 65.43% at 40 mA. The efficiency droop of 3.848% is observed in LED₃ at 40 mA. The partial strain relaxation inside the active region is primarily responsible for the enhancement of

EQE in case of prestrain structures. As a result, there is a reduced band-edge tilt in each well and the overlap between the carrier wave functions is improved. It means that the PZ field can be efficiently minimized by adding prestrain interlayer inside the structure. Thus the proposed nanowire structure obtains an enhanced luminescence which can benefit the light industry.

3.2 | Luminous power

Figure 4 illustrates the calculated optical power at 300 K for the designed LED samples. At 40 mA, LED nanowires have their output powers as 3.12 mW, 5.74 mW, and 9.77 mW thus showing a superior power in LED₃ compared to the remaining structures. Our proposed device has also obtained better optical power compared to some of the previously mentioned studies. This enhancement in the power of LED₂ and LED₃ is due to the residual strain release, reduction of PZ and Stark effect, improvement of recombination rate and crystal quality in MQWs, and, thus, results in enhanced luminescence.

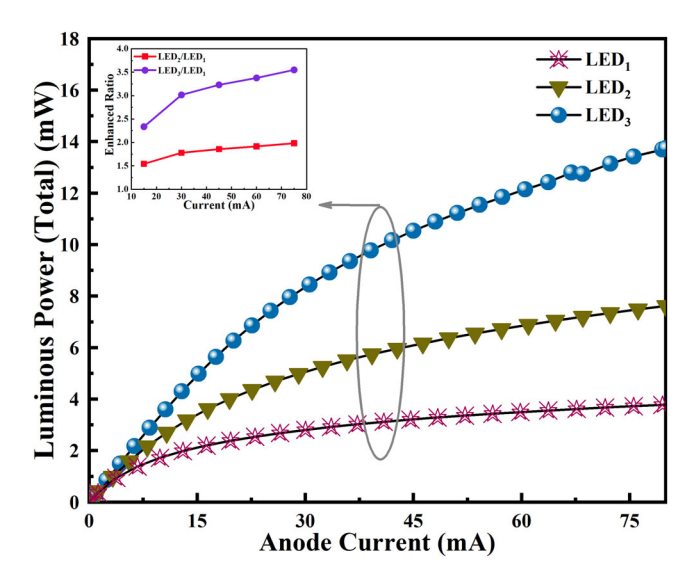


FIGURE 4 Optical power of light emitting diode (LED) samples (L-I curve). Inset shows the enhanced ratio, that is, optical power of the proposed sample (LED₂ and LED₃) divided by regular (LED₁).

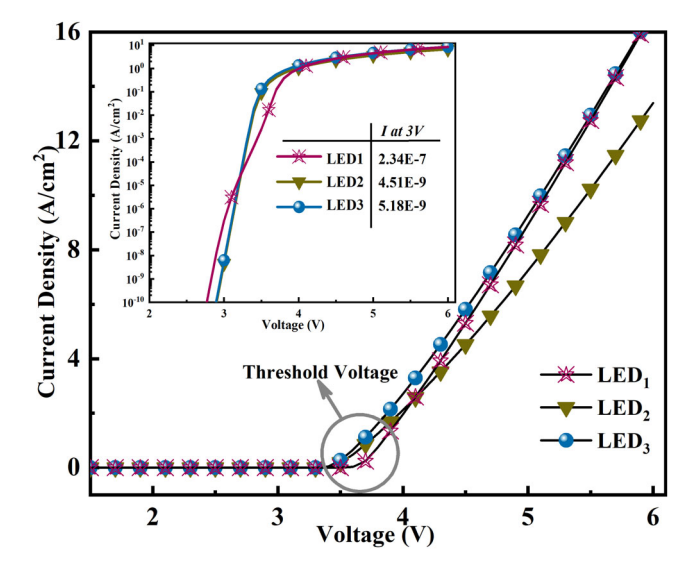


FIGURE 5 I-V characteristics of all light emitting diodes (LEDs). Inset illustrates I-V curves in a logarithmic scale. The calculated currents at 3 V are listed in the inset.

10991204, 2024, 2, Downloaded from https://onlinelibrary.wiley.com/doi/10.1002/jmm.3169 by National Yang Ming Chiao Tung University, Wiley Online Library on [30/06/2024]. See the Terms

3.3 | I-V characteristics

I-V characteristics for the three samples of LED are shown in Figure 5. The figure depicts that the proposed LED has a lower threshold voltage compared to the others. The heterointerface of the EBL and QW exhibits band bending in the valence band, as seen from Figure 2A. This phenomena raises the turn-on voltage for LED $_1$ and LED $_2$ and lowers the hole injection efficiency in the wells. In LED $_3$, the series resistance is also reduced, showing a considerable improvement in the transmission of holes.

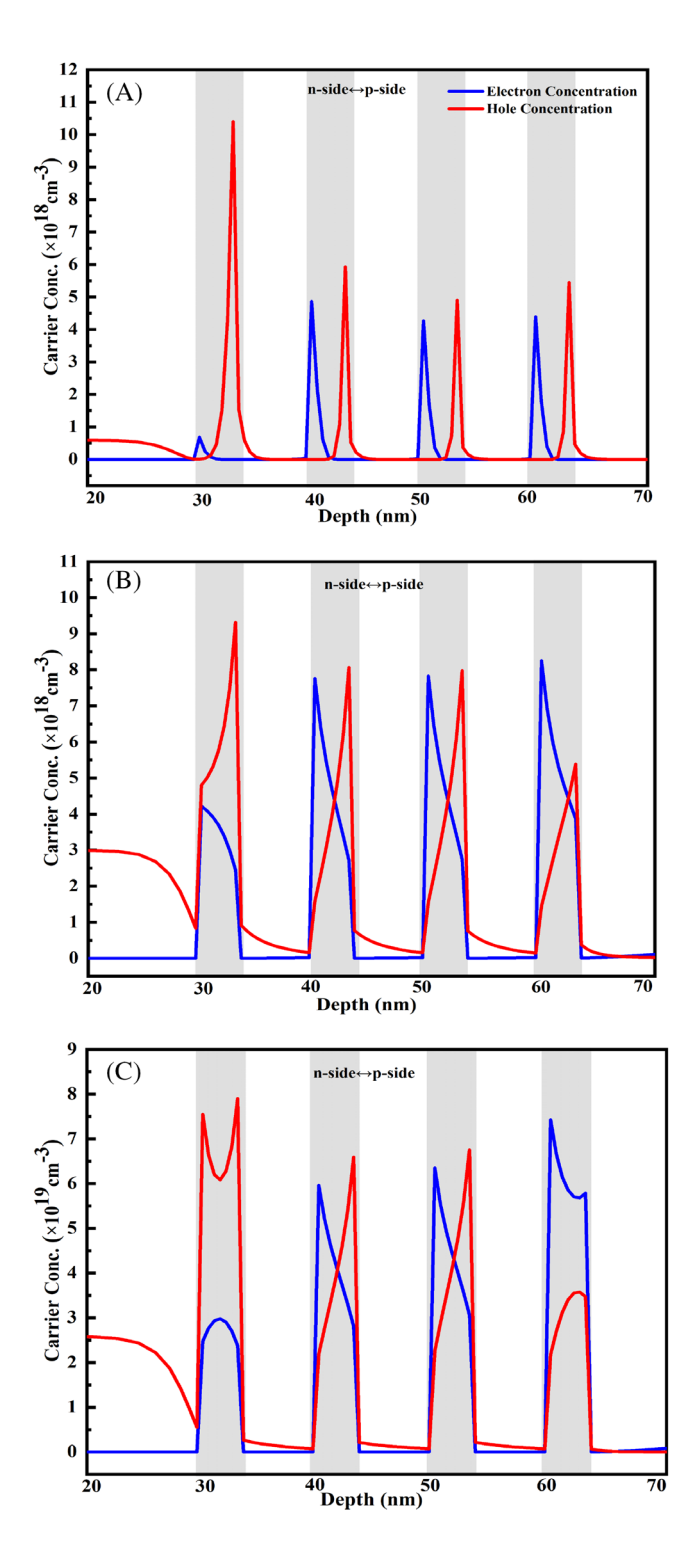


FIGURE 6 Carrier concentration of (A) LED₁, (B) LED₂, and (C) LED₃.

3.4 | Carrier concentration

The carrier concentration of LED_1 , LED_2 , and LED_3 at 40 mA is illustrated in Figure 6. In presence of prestrain layers, it indicates evident electron homogeneity because of the tilted band profile. The better electron confinement leads to remarkable reduction of electron leakage into the p-region as displayed, and thus has superior carrier concentration. Due to the absence of EBL in LED_3 , electrons are confined in the active region. Thus, there is minimum electron leakage in LED_3 , as shown in Figure 7.

3.5 | Recombination rate

Because of larger current densities in the active region and minimum electron leakage of LED₃, it possesses larger radiative recombination as shown in Figure 8. The degree of overlap between electrons and holes increases which eventually enhances the rate of radiative recombination for the proposed device LED₃.

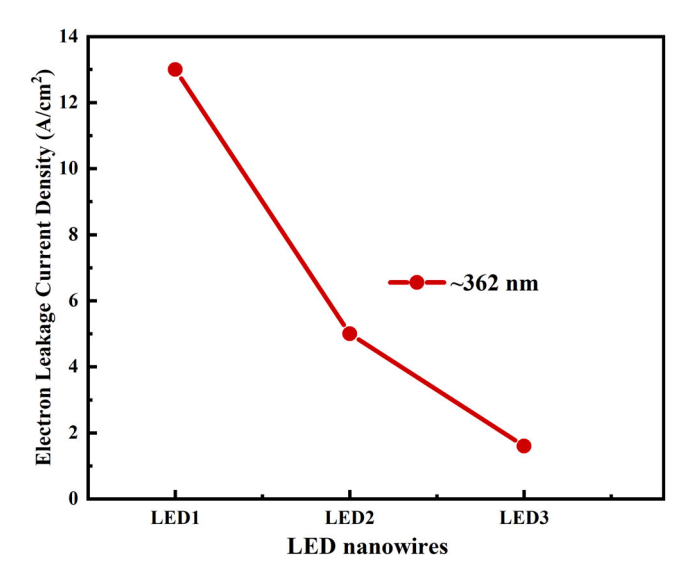


FIGURE 7 Electron leakage current density for all the three designed light emitting diodes (LEDs).

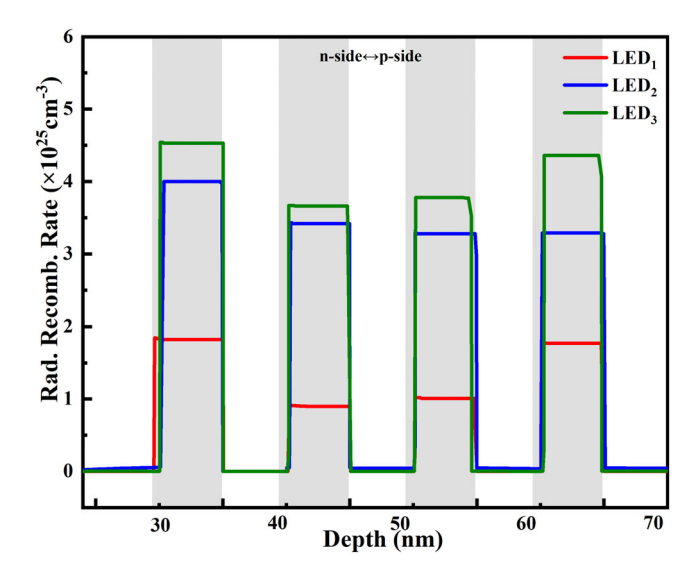


FIGURE 8 Radiative recombination rate of all the three designed light emitting diodes (LEDs).

3.6 Power spectral density

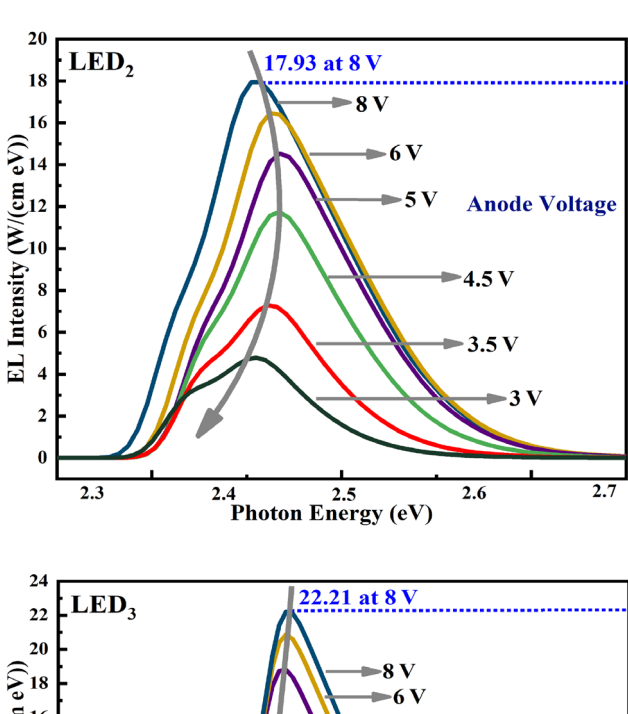
WILEY

The electroluminescence (EL) spectra of all the samples are shown in Figure 9 within a voltage range from 3 to 8 V. The proposed structure LED₃ numerically accomplishes 23.8% higher peak intensity than LED₂ at 8 V.

For LED₂, the EL spectra shows a blue-shift with decreasing bias voltage, later on toward red-shift shown in Figure 9A. The PZ field is compensated by applied electric field hence the QCSE decreases along with a blue-shift. When PZ field is of same value as the applied electric field, then the flat-band condition is obtained under which the PL peak reaches the highest value. On further decreasing the bias voltage, the net electric field in the active region is inverted and we observe a red-shift. The presence of low blue-shift is indicated in LED₃. The dependency of energy band-gap on temperature is demonstrated by using Varshni's formula as follows:

$$E_g = E_{g(T=0K)} - \frac{\alpha T^2}{T + \beta},$$

where α and β are fitting parameters, also known as Varshni's parameters. ²² This equation signifies a decrease of energy band gap with rising temperature, hence the overall emission wavelength shifts to a higher value. This is the reason due to which the overall emission shifts to a longer value with increase in temperature. According to Varshni's law, the increase in temperature leads to a narrow energy band gap of QW.²² Initially the wavelength shifts toward a lower value with increase in current, termed as blue-shift, which is caused due to the screening effect. However, with further increase in current, the wavelength shifts to a longer value known as red-shift. This is caused by thermal effect formed



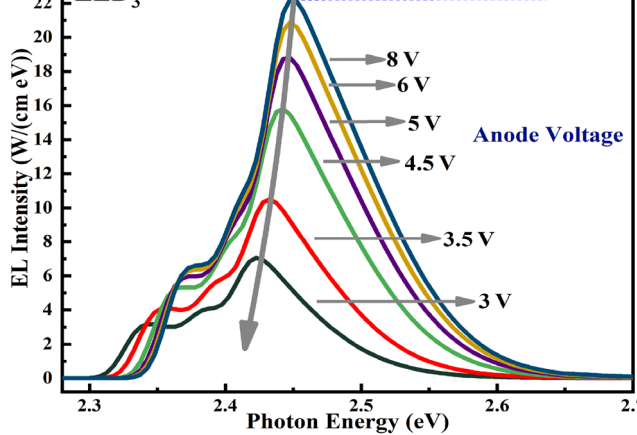


FIGURE 9 Room temperature electroluminescence (EL) spectra of (A) LED₂ and (B) LED₃ as a function of applied bias voltage.

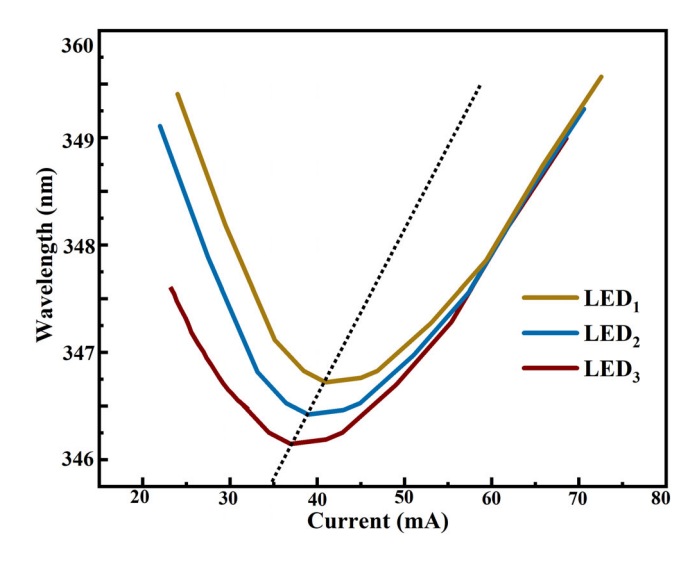


FIGURE 10 Emission wavelengths as a function of injection currents for all the three designed light emitting diodes (LEDs).

TABLE 3 Optimized performance parameters of the proposed structure.

Parameters	LED_1	LED_2	LED_3
Electron concentration (cm ⁻³) at 2nd QW	4.86×10^{18}	7.754×10^{18}	5.95×10^{19}
Hole concentration (cm ⁻³) at 2nd QW	5.93×10^{18}	8.064×10^{18}	6.591×10^{19}
EQE (%) at 40 mA	20.95	38.16	65.43
Droop (%)	29.56	9.306	3.848
Power (mW)	3.12	5.74	9.77
Current density (A/cm ²)	9.26	7.24	10.3
Recombination rate at 2nd QW (cm ⁻³ s ⁻¹)	16.3×10^{25}	32.7×10^{26}	51.1×10^{26}

Abbreviations: LED, light emitting diode; QW, quantum well.

by parasitic resistances at which there is a transition from blue toward red shift, drawn out from the dotted lines of Figure 10. It can be noticed that the conventional LED has larger slope than ones with prestrain interlayer. The currents during the transition of wavelength of LED₁, LED₂, and LED₃ are 42.3, 39.9, and 33.5 mA, respectively at room temperature which indicates a strong PZ field in LED₁. Hence, it will require more injection carrier, that is, higher current to fulfill QSCE screening with the active region.

Finally, the calculated parameters of the conventional and proposed LED nanowires are listed in Table 3. Thus, our work presents a method to show the comparison of electrical and optical parameters within the MQW region of EBL free InGaN LED and how it has been affected with varying indium composition in the InGaN/GaN prestrained layers.

4 | CONCLUSION

The impact of prestrained layer on the device parameters of an EBL free GaN/InGaN LED is investigated. In the proposed device the strain is more relaxed as compared to LED₂. It indicates poor QSCE in LED₃ and thus obtains a higher efficiency of 65.43% at an injection current of 40 mA and weaker efficiency droop of 3.848%. At constant bias of 8 V, LED₃ accomplishes 23.8% higher output power than LED₂. The radiative recombination rates are higher with the prestrained interlayer. Also, the wavelength-current measurement shows that the proposed device LED₃ has low blue-shift compared to the remaining structures. Therefore, a higher PZ field has to be effectively screened while inserting enough carriers. The proposed device has a huge contribution toward strain release and minimizes QCSE which leads to enhanced luminescence.



AUTHOR CONTRIBUTIONS

All authors equally contributed for the preparation of the manuscript.

ACKNOWLEDGEMENTS

This work is the outcome of DST-SERB, Government of India sponsored MATRICS Project No MTR/2021/000370 which is duly acknowledged for kind support.

CONFLICT OF INTEREST STATEMENT

The authors declare that they have no known competing financial interests or personal relationships that could have appeared to influence the work reported in this paper. This article does not contain any study on human beings or animals.

DATA AVAILABILITY STATEMENT

The data that support the findings of this study are available from the corresponding author upon reasonable request.

CONSENT FOR PUBLICATION

All authors have given consent for publication.

ORCID

Samadrita Das https://orcid.org/0000-0001-8624-2171

Trupti Ranjan Lenka https://orcid.org/0000-0002-8002-3901

Hieu Pham Trung Nguyen https://orcid.org/0000-0003-1129-9581

Giovanni Crupi https://orcid.org/0000-0002-6666-6812

REFERENCES

- 1. Bui HQT, Velpula RT, Jain B, et al. Full-color InGaN/AlGaN nanowire micro light-emitting diodes grown by molecular beam epitaxy: a promising candidate for next generation micro displays. *Micromachines*. 2019;10(8):41034-41040. doi:10.3390/mi10080492
- 2. Chan L, Karmstrand T, Chan A, et al. Fabrication and chemical lift-off of sub-micron scale III-nitride LED structures. *Opt Express*. 2020; 28(23):35038-35046. doi:10.1364/oe.403299
- 3. Tsai CL, Wang TW, Li YC, et al. Underwater optical wireless communications with InGaN LEDs grown with an asymmetric multiple quantum well for light emission or detection. *IEEE Photonics J.* 2022;14(1):1-7. doi:10.1109/JPHOT.2021.3130133
- 4. Guo L, Guo Y, Yang J, et al. 275 nm deep ultraviolet AlGaN-based micro-LED arrays for ultraviolet communication. *IEEE Photonics J*. 2022;14(1):1-5. doi:10.1109/JPHOT.2021.3129648
- 5. Pawlikowski W, Barmaki A, Narimani M, Hranilovic S. Light-emitting commutating diodes for optical wireless communications within LED drivers. *IEEE Photonics J.* 2020;12(5):1-11. doi:10.1109/JPHOT.2020.3020749
- 6. Hsu CW, Yeh CH, Chow CW. Using adaptive equalization and polarization-multiplexing technology for gigabit-per-second phosphor-LED wireless visible light communication. Opt Laser Technol. 2018;104:206-209. doi:10.1016/j.optlastec.2018.02.004
- 7. Jeong H, Jeong SY, Park DJ, et al. Suppressing spontaneous polarization of p-GaN by graphene oxide passivation: augmented light output of GaN UV-LED. *Sci Rep.* 2015;5:1-6. doi:10.1038/srep07778
- 8. Das S, Lenka TR, Talukdar FA, et al. Effects of polarized-induced doping and graded composition in an advanced multiple quantum well InGaN/GaN UV-LED for enhanced light technology. *Eng Res Express*. 2022;4(1):015030-015041. doi:10.1088/2631-8695/ac4fb1
- 9. Kwon SY, Kim HJ, Na H, et al. In-rich InGaN/GaN quantum wells grown by metal-organic chemical vapor deposition. *J Appl Phys.* 2006;99(4):1-6. doi:10.1063/1.2173043
- 10. Bernardini F, Fiorentini V, Vanderbilt D. Spontaneous polarization and piezoelectric constants of III-V nitrides. *Phys Rev B Condens Matter Mater Phys.* 1997;56(16):R10024-R10027. doi:10.1103/PhysRevB.56.R10024
- 11. Zhang ZH, Liu W, Ju Z, et al. Self-screening of the quantum confined Stark effect by the polarization induced bulk charges in the quantum barriers. *Appl Phys Lett.* 2014;104(24):16-21. doi:10.1063/1.4883894
- 12. Dadgar A, Groh L, Metzner S, et al. Green to blue polarization compensated c-axis oriented multi-quantum wells by AlGaInN barrier layers. *Appl Phys Lett.* 2013;102(6):356-362. doi:10.1063/1.4793185
- 13. Huang H-M, Lu T-C, Chang C-Y, et al. Investigation of emission polarization and strain in InGaN/GaN multiple quantum wells on nanorod epitaxially lateral overgrowth templates. 2012;8262:82621Y. doi:10.1117/12.906635
- 14. Huang CF, Liu TC, Lu YC, et al. Enhanced efficiency and reduced spectral shift of green light-emitting-diode epitaxial structure with prestrained growth. *J Appl Phys.* 2008;104(12):9430-9437. doi:10.1063/1.3046582
- 15. Das S, Lenka TR, Talukdar FA, Velpula RT, Nguyen HPT, Crupi G. Influence of prestrained graded InGaN interlayer on the optical characteristics of InGaN/GaN MQW-based LEDs. pp. 91–92, 2022. 10.1109/NUSOD54938.2022.9894827
- 16. Clara S. Silvaco User's manual DEVICE SIMULATION SOFTWARE. 2004 www.silvaco.com

- 17. Ambacher O, Majewski J, Miskys C, et al. Pyroelectric properties of Al(In)GaN/GaN hetero- and quantum well structures. *J Phys Condens Matter*. 2002;14(13):3399-3434. doi:10.1088/0953-8984/14/13/302
- 18. Karpov S. ABC-model for interpretation of internal quantum efficiency and its droop in III-nitride LEDs: a review. *Opt Quantum Electron*. 2015;47(6):1293-1303. doi:10.1007/s11082-014-0042-9
- 19. Bui HQT, Velpula RT, Jian B, et al. High-performance nanowire ultraviolet light-emitting diodes with potassium hydroxide and ammonium sulfide surface passivation. *Appl Optics*. 2020;59(24):7352-7356. doi:10.1364/ao.400877
- 20. Yan L, Zhang Y, Han X, et al. Polarization-induced hole doping in N-polar III-nitride LED grown by metalorganic chemical vapor deposition. *Appl Phys Lett.* 2018;112(18):8123-8131. doi:10.1063/1.5023521
- 21. Zettler JK, Hauswald C, Corfdir P, et al. High-temperature growth of GaN nanowires by molecular beam epitaxy: toward the material quality of bulk GaN. *Cryst Growth Des.* 2015;15(8):4104-4109. doi:10.1021/acs.cgd.5b00690
- 22. Ravindra NM, Srivastava VK. Temperature dependence of the energy gap in semiconductors. *J Phys Chem Solid.* 1979;40(10):791-793. doi:10.1016/0022-3697(79)90162-8

How to cite this article: Das S, Lenka TR, Talukdar FA, Nguyen HPT, Crupi G. The role of indium composition in $In_xGa_{1-x}N$ prestrained layer towards optical characteristics of EBL free GaN/InGaN nanowire LEDs for enhanced luminescence. *Int J Numer Model.* 2024;37(2):e3169. doi:10.1002/jnm.3169